Modeling and Control of Doubly Fed Induction (DFIG) Wind energy conversion system

H. Abouobaida, M. Cherkaoui

Department of Electrical Engineering,
Ecole Mohammadia d'ingénieurs, Mohammed V University, Rabat, Morocco
Hassanabouobaida@gmail.com, cherkaoui@emi.ac.ma

Abstract **- This paper presents a control strategy for a grid connected doubly fed induction generator (DFIG)-based wind energy conversion system. Control strategies for the grid side and rotor side converters placed in the rotor circuit of the DFIG are presented along with the mathematical modeling of the employed configuration. The maximum power point extraction of the wind turbine, unity power factor operation of the DFIG are also addressed along with the proposed strategy. The developed approach control is then simulated in MATLAB-SIMULINK and the developed model is used to illustrate the behavior of the system. The simulation results are presented and discussed at the end of this paper.**

Index Terms - D**oubly fed induction generator (DFIG), grid power, unity power factor, wind energy conversion system, modeling, converters.**

I. INTRODUCTION

The growing need for electrical energy and the will to preserve the nature justifies the use of renewable energy sources**.** The use of renewable sources for electric power generation has been a huge increase since the past decade. Increased economical and ecological woes have driven researchers to discover newer and better means of generating electrical energy. In this race, the production of electricity by wind turbine is actually the best method in comparison with the energy produced by the solar source conversion and this is due to the price per a kilo watt that is less elevated with respect to the second [1]. Among the most used and available technologies for wind turbines, the doubly fed induction generator (DFIG) is the most accepted because it presents greater benefits for a reduced conversion structure of wind turbine based on a conversion (DFIG). The doubly fed induction generator is the most popular option for harnessing energy from the wind because of variable and unpredictable nature of the wind speed. This base structure (DFIG) offers the benefits of improved efficiency, reduced converter, cost and losses are reduced, easy implementation of power factor correction, a variable speed operation, and the control four quadrants of active and reactive power. Due to variable speed operation, the total energy production is 20% to 30% higher and therefore capacity utilization factor is improved and the cost per kWh of energy is reduced.

In general, the stator windings of the DFIG are directly connected the electrical network and the rotor windings are powered via bidirectional PWM voltage converters (VSC). The control strategy is used to control the rotor and the stator output power supplied to the grid variable speed operation [2].

Decoupled control of active and reactive powers is the used approach based on vector control. Transfer of active power by a wind turbine based on (DFIG) in the distribution network can be carried out by the stator and rotor. The transfer direction of the active power is determined by wind speed and hence the synchronous speed of the generator. When a speed of the generator below the synchronous speed then the transfer of active power flows from the network to the electric rotor machine. The transfer is made by two cascaded converters. The first is linked to the network operates as a rectifier and the second operates as an inverter is connected to the rotor of the generator.

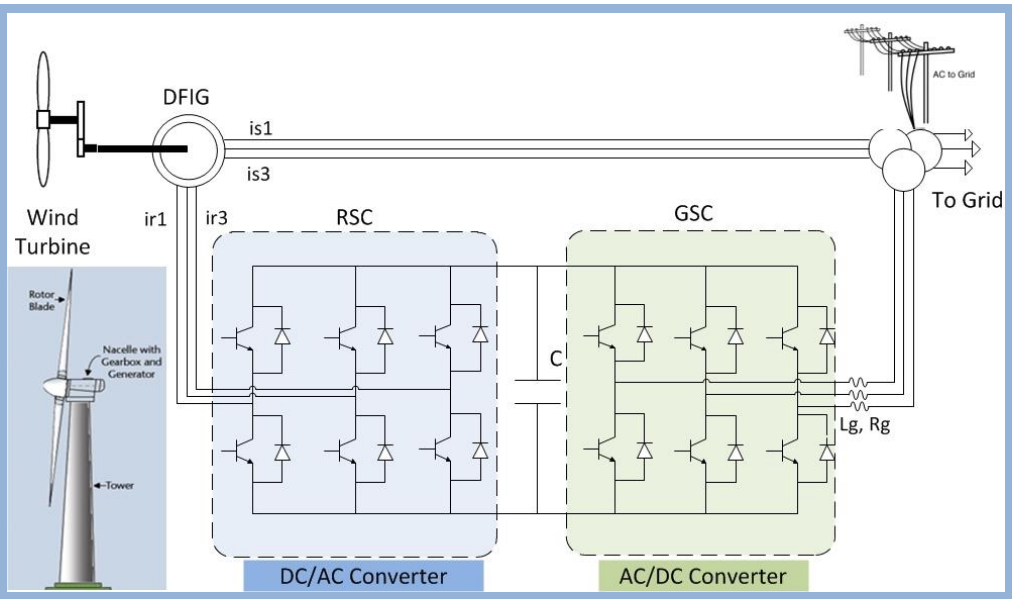

Fig 1 : DFIG-based Wind energy conversion system

The Wind energy conversion system configuration used in this work (DFIG with converters cascade and a capacity energy storage system in the dc link) is shown in Fig. 1.

This paper is structured as follows. Section II presents the modeling of the DFIG system. The detailed control strategy is discussed in Section III. Section IV presents and discusses simulation and results followed by conclusions in Section V.

II. Wind energy conversion system modeling

The wind turbine modeling is inspired from [3]. In the following, the wind turbine components models are briefly described.

a) *The Turbine Model*

The aerodynamic power *P* captured by the wind turbine is given by :

$$P = \frac{1}{2}\pi\rho R^2 Cp(\lambda)v^3 \qquad (1)$$

Where the tip speed ratio λ is given by :

$$\lambda = \frac{R\omega}{v} \qquad (2)$$

and *v* is the wind, ρ is the air density, *R* is the rotor radius, and *Cp* is the power coefficient.

λ is the ratio of turbine blades tip speed to wind speed and β is the turbine blades rotational speed. In a wind turbine, C_p can be represented by a nonlinear curve in terms of λ in place of different β as illustrated in Fig 2:

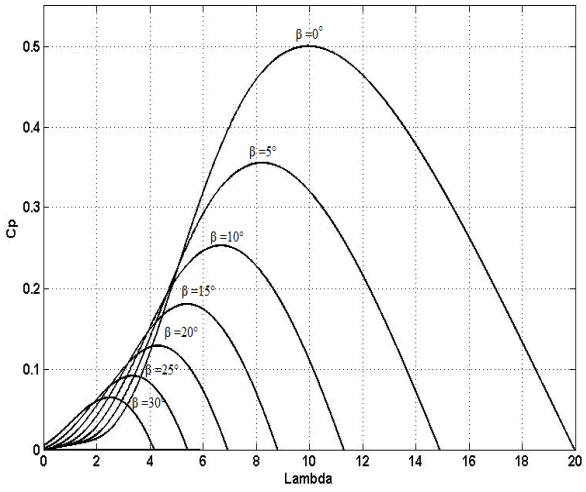

Fig 2 : Curve of Cp in function of λ for different value of the Pitch angle β

The rotor power (aerodynamic power) is also defined by *:*

$$P = T_m \cdot \omega \qquad (3)$$

where *Tm* is the aerodynamic torque and ω is the wind turbine rotor speed.

The following simplified model is adopted for the turbine :

$$J\frac{d\omega}{dt} = T_m - T_{em} - K.\omega \qquad (4)$$

where *Tem* is the generator electromagnetic torque, J is the turbine total inertia, and K is the turbine total external damping.

The active and reactive stator and rotor powers are expressed by:

$$\begin{cases} P_s = V_{sd}I_{sd} + V_{sq}I_{sq} \\ Q_s = V_{sq}I_{sd} - V_{sd}I_{sq} \\ P_r = V_{rd}I_{rd} + V_{rq}I_{rq} \\ P_r = V_{rq}I_{rd} - V_{rq}I_{rq} \end{cases} \qquad (5)$$

To improve system efficiency, turbine speed is adjusted as a function of wind speed to maximize output power. Operation at the maximum power point can be realized over a wide power range. Fig. 2 illustrates typical output power-speed curves as a function of turbine speed and wind speed [4].

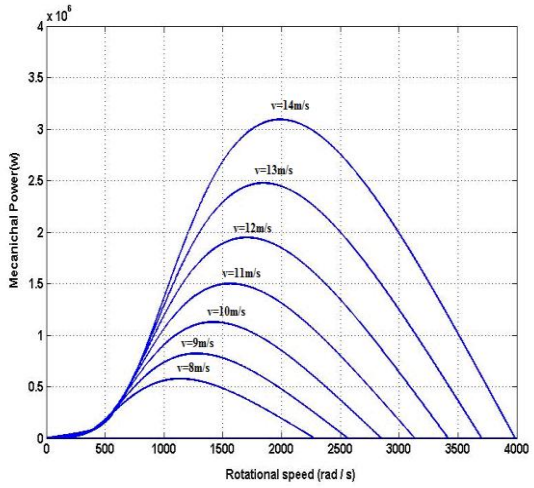

Fig 3 : Electrical output power as a function of turbine speed. Parameter curves are plotted for different wind speeds.

b) The DFIG Model

The control system is usually defined in the synchronous *d-q* frame fixed to either the stator voltage or the stator flux [5]. For the proposed control strategy, the generator dynamic model written in a synchronously rotating frame *d-q* is given by:

$$\begin{cases} V_{sd} = R_s\, I_{sd} + \frac{d\Phi_{sd}}{dt} - \omega_s.Isq \\ V_{sq} = R_s\, I_{sq} + \frac{d\Phi_{sq}}{dt} + \omega_s.I_{sd} \\ V_{rd} = R_r\, I_{rd} + \frac{d\Phi_{rd}}{dt} - \omega_r.I_{rq} \\ V_{rq} = R_r\, I_{rq} + \frac{d\Phi_{rq}}{dt} + \omega_r.I_{rd} \\ T_{em} = P\,M\left(I_{rd}\, I_{sq} - I_{rq}.I_{sd}\right) \\ \Phi_{sd} = L_s\, I_{sd} + m.L_m.I_{rd} \\ \Phi_{sq} = L_s\, I_{sq} + m.L_m.I_{rq} \\ \Phi_{rd} = L_r\, I_{rd} + m.L_m.I_{sd} \\ \Phi_{rq} = L_r\, I_{rq} + m.L_m.I_{sq} \end{cases} \qquad (6)$$

where V is the voltage, I the current, Φ is the flux, R is the resistance, L is inductance, M is the mutual inductance, T_{em} is the electromagnetic torque, and P is the pole pair number.

c) Modeling of GSC and Grid

In this section, we focus on the modeling of the AC/DC converter connected to power grid via the RL filter as illustrated in Figure 4.

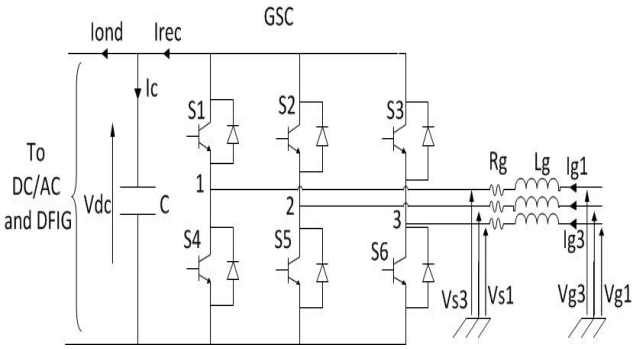

Fig 4 : Grid connected to AC/DC converter

The model of the three-phase grid connected AC/DC converter is presented by the following equations:

$$\begin{cases} \frac{CdVdc}{dt} = Irec - Iond \\ Vs1 = Vg1 - Rg.Ig1 - Lg.\frac{dIg1}{dt} \\ Vs2 = Vg2 - Rg.Ig2 - Lg.\frac{dIg2}{dt} \\ Vs3 = Vg3 - Rg.Ig3 - Lg.\frac{dIg3}{dt} \end{cases} \qquad (7)$$

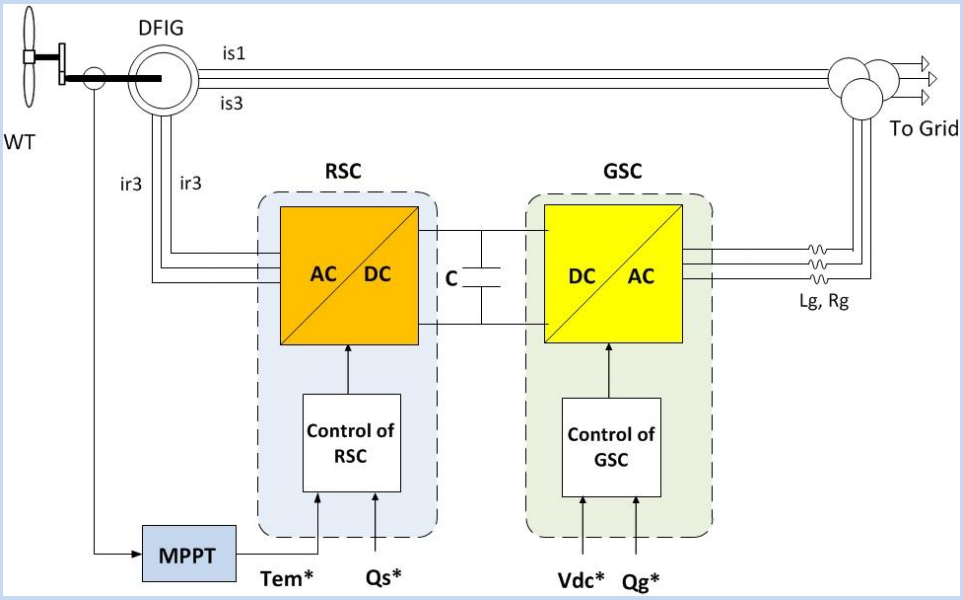

Fig 5 : Control strategy of wind energy conversion system

With
Vgi : voltages of the electrical network,
Igi : currents of electrical network,
Irec, Iond : output current of the AC/DC converter and input current of the DC/AC converter respectively,
Vdc, Ic : voltage and current of the DC link capacitor respectively
Vsi : input voltages of the AC/DC converter
Si : IGBT transistor

III. *Control Strategy*

The architecture of the controller is shown in Figure 5. It is based on the three-phase model of the electromechanical conversion chain of the wind system [6].

The control strategy has three objectives:
- Control of extraction of maximum wind power using "MPPT" (Maximum Power Point Tracking),

- Control of the RSC by controlling the electromagnetic torque and reactive power of stator of DFIG,

- Control of the GSC by controlling the DC bus voltage, active and reactive power exchanged with the network.

a) MPPT strategy :

Figure 6 shows the principle of MPPT control of wind turbine without control of the rotation speed [7]. The control objective is to optimize the capture wind energy by tracking the optimal torque *Tem**.

$$T_{em} *= k.\omega_m{}^2 \qquad (8)$$

With $k = \frac{1}{2}.\pi.\rho.R^5.\frac{Cp_{max}}{\lambda_{opt}^3}$

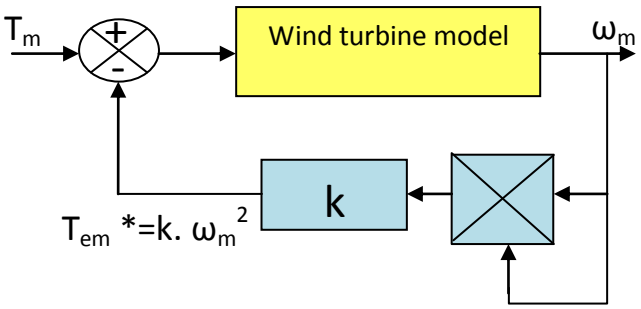

Fig 6 : MPPT control strategy

b) Control of the DC/AC converter

Controls the electromagnetic torque and stator reactive power will be obtained by controlling the dq-axes rotor currents of the DFIG.

The stator field rotates in steady state at the synchronous speed. This field is symbolized by the stator flux vector which gives a visual idea of the phase and flux amplitude. By choosing the two-phase dq related to rotating stator field, and placing the stator flux vector on the d-axis, we can write [8]:

$$\begin{cases} \Phi sd = \Phi s \\ \Phi sq = 0 \end{cases} \quad (9)$$

Considering the choice of reference related to dq rotating stator field and neglecting the resistance of the stator windings, a simplification of the equations of DFIG in the dq reference can be obtained from equation (6):

$$\begin{cases} V_{sq} = \omega_s \Phi_{sd} \;\; ; \;\; V_{sd} = 0 \\ V_{rd} = R_r\, I_{rd} + \frac{d\Phi_{rd}}{dt} - \omega_r\, I_{rq} \\ V_{rq} = R_r\, I_{rq} + \frac{d\Phi_{rq}}{dt} + \omega_r\, I_{rd} \end{cases} \quad (10)$$

From the equations (6) of the stator and rotor flux in dq axes, the stator currents can be obtained from the following expressions:

$$\begin{cases} I_{sd} = \frac{\Phi_{sd} - m.L_m.I_{rd}}{L_s} \\ I_{sq} = \frac{m.L_m}{L_s}.I_{rq} \end{cases} \quad (11)$$

These expressions are then substituted into the equations (6) of the rotor flux which then become:

$$\begin{cases} \Phi_{rd} = \left(L_r - \frac{(m.L_m)^2)}{L_s}\right).I_{rd} + \frac{m.L_m}{L_s}.\Phi_{sd} \\ \Phi_{rq} = L_r.I_{rq} - \frac{(m.L_m)^2}{L_s}\, I_{rq} = L_r.\sigma.I_{rq} \end{cases} \quad (12)$$

With :

$\sigma = 1 - \frac{(m.Lm)^2}{L_s L_r}$ is the dispersion coefficient of the DFIG.

By replacing the expressions of direct and quadrature components of rotor flux (12) in equations (10), we obtain:

$$\begin{cases} V_{rd} = R_r\, I_{rd} + Lr.\sigma.\frac{dI_{rd}}{dt} + e_{rd} \\ V_{rq} = R_r\, I_{rq} + Lr.\sigma.\frac{dI_{rq}}{dt} + e_{rq} + e_{\Phi} \end{cases} \quad (13)$$

Where:

$$\begin{cases} e_{rd} = -\sigma.L_r.\omega_r.I_{rq} \\ e_{rq} = -\sigma.L_r.\omega_r.I_{rd} \\ e_{\Phi} = \omega_r.\frac{m.L_m}{L_s}.\Phi_{sd} \end{cases} \quad (14)$$

The electromagnetic torque Tem can be expressed from the flux and the stator currents by:

$$T_{em} = P.(\Phi_{sd}.I_{sq} - \Phi_{sq}.I_{sd}) \quad (15)$$

It can also be expressed in terms of the rotor currents and stator flux:

$$T_{em} = P.\frac{m.L_m}{L_s}(\Phi_{sq}.I_{rd} - \Phi_{sd}.I_{rq}) \quad (16)$$

From equation (9), the electromagnetic torque becomes:

$$T_{em} = -P.\frac{m.L_m}{L_s}.\Phi_{sd}.I_{rq} \quad (17)$$

The active and reactive stator powers are expressed by:

$$\begin{cases} P_s = -V_{sq}.\frac{m.L_m}{L_s}.\Phi_{sd}.I_{rq} \\ Q_s = V_{sq}.\frac{V_{sq}.\Phi_{sd}}{L_s} - \frac{m.L_m}{L_s}.V_{sq}I_{rd} \end{cases} \quad (18)$$

Expressions (17) and (18) show that in the case where the stator flux Φ_{sq} is kept constant (this condition is ensured in the case of a stable network connected to the stator of the DFIG), the choice of dq reference makes the electromagnetic torque produced by the DFIG, and therefore the stator power will be proportional to the q-axis rotor current. Reactive stator power is not proportional to the d-axis rotor current due to constant imposed by the network. Thus, the reactive stator power can be controlled independently [9].

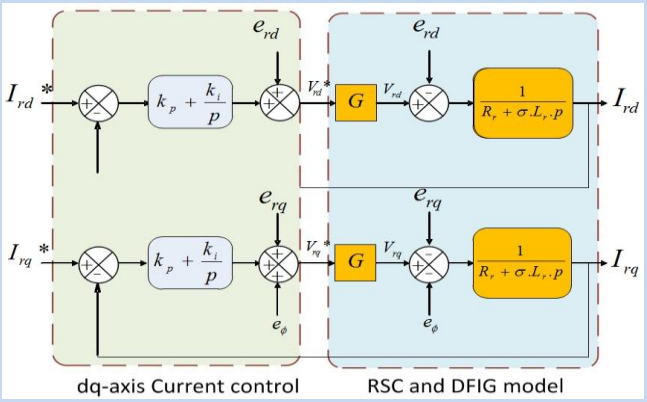

Fig 7 : dq-axis rotor current control

The DFIG model in dq reference related to stator rotating field shows that we can establish a rotor currents control given that
the influence of couplings can be controlled of each current independently. The reference values for these regulators will be the q-axis rotor current and the d-axis rotor current.

To establish control loops of the rotor currents, we assume that the RSC (rotor side converter) is ideal (which corresponds to neglecting the dead time imposed by the drivers of the power switches) and using the state averaging method, the DC/AC converter (RSC) may be represented by a gain G whose expression is:

$$G = \frac{V_{dc}}{2.V_p} \qquad (19)$$

with:
V_p: the amplitude of the triangular carrier of the generation of the PWM.
V_{dc} : voltage of the DC link capacitor.

Furthermore, we assume that the rotor voltages are equal to their references V_{rk}* ($k \in \{1, 2, 3\}$), which means that the amplitude V_p of the carrier must be secured to V_{dc} / 2, implying a gain G = 1.

The block control loops of the dq axes rotor currents diagram is shown in Figure 7. The controllers used are PI correctors.

The reference of the q-axis rotor current is derived from the MPPT control via reference of electromagnetic torque (Equation 17 and 8).

The reference current of the d-axis rotor current is derived from the control of the stator reactive power.

Figure 8 shows the control block diagram of the RSC. This approach can independently control the dq axis rotor currents and therefore active and reactive power of the stator.

To generate the reference current of the rotor, it is necessary to estimate the stator flux according to the d-axis. In our study, the grid is assumed to be stable and the dq reference chosen is related to the stator rotating field. Thus, the d-axis stator flux can be estimated from measurements of the d-axis stator and rotor currents in open loop :

$$\Phi_{sd-est} = L_s I_{sd} + m.L_m.I_{rd} \qquad (20)$$

Once the stator flux is estimated, it is necessary to generate the dq-axes rotor reference currents. The electromagnetic torque is proportional to the q-axis rotor current (according to Equation 17), so we can establish a relation between the i_{rq}* current and the electromagnetic torque T_{em}* from block MPPT control by:

$$I_{rq}* = \frac{L_s}{P.m.L_m\Phi_{sd\_est}}.T_{em} \qquad (21)$$

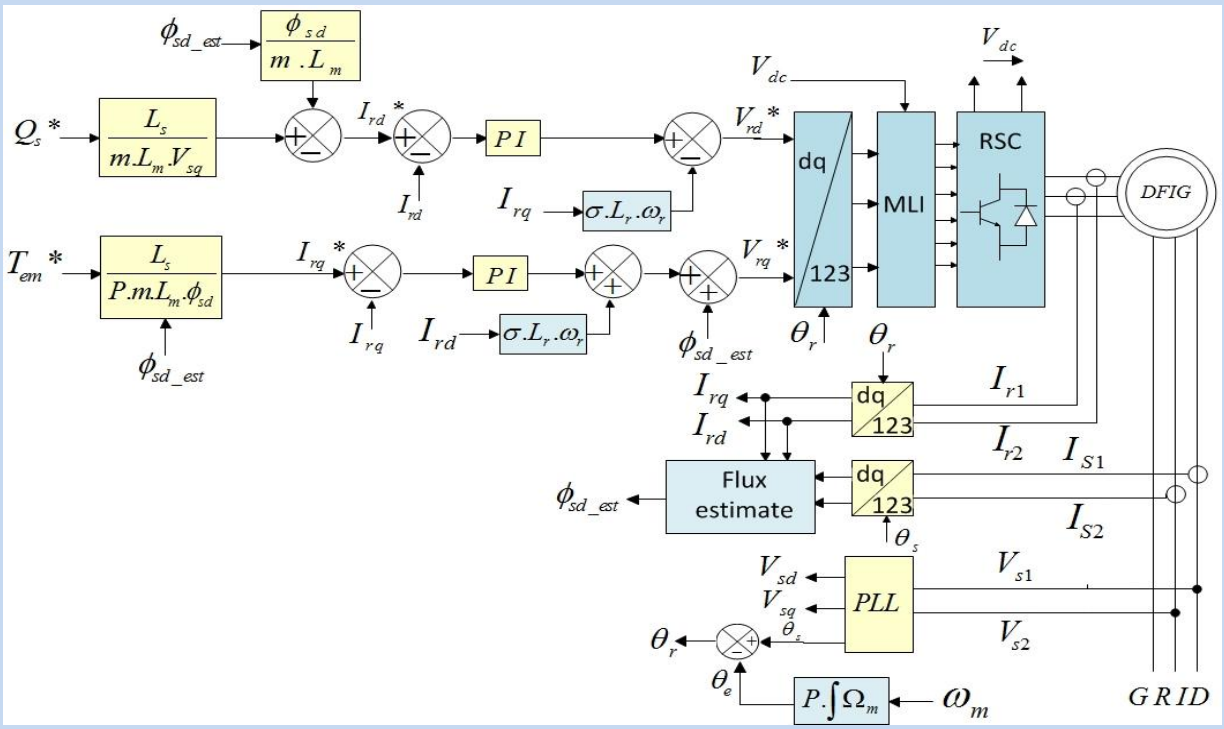

FIG 8 : Control approach of the Rotor Side Converter (RSC)

Regarding the rotor d-axis current reference, two methods are developed in the literature:
- This current is established to control the reactive stator power,
- This current is established to minimize the Joule losses in the rotor and stator.

In the context of this paper, we retain the first solution because we have chosen to control the value of the reactive power.

$$I_{rd}* = \frac{\Phi_{sd\_est}}{m.L_m} - \frac{L_s}{m.L_m.V_{sq}}.Q_s* \quad (22)$$

c) Control of the AC/DC converter

The GSC (Grid Side Converter) is AC/DC converter connected between the DC bus and the electrical network via a RL filter. This converter has two roles:

- Maintain the DC bus voltage constant, regardless of the magnitude and direction of flow of the rotor power of the DFIG,
- Maintain a unity power factor at the point of connection to the electricity grid.

Figure 9 describes the command of the AC/DC converter. This command performs the following two functions:
- Control of the currents flowing in the RL filter,
- Control of the DC bus voltage.

In the dq reference related stator rotating field, equation (7) becomes:

$$\begin{cases} V_{sd} = V_{gd} - R_g.I_{gd} - L_g.\frac{dI_{gd}}{dt} + e_{gd} \\ V_{sq} = V_{sq} - R_g.I_{gq} - L_g.\frac{dI_{gq}}{dt} + e_{gq} \end{cases} \quad (23)$$

With :

$$\begin{cases} e_{gd} = \omega_s.L_g.I_{gq} \\ e_{gq} = V_{gd} - \omega_s.L_g.I_{gd} \end{cases} \quad (24)$$

Modeling of the connection of the AC/DC converter (GSC) to the network in the following rotating dq stator field reference shows that we can set up a control of the current flowing through the RL filter, and the influence couplings near each axis can be controlled independently. The magnitudes for these regulators are RL filter in dq axes currents.

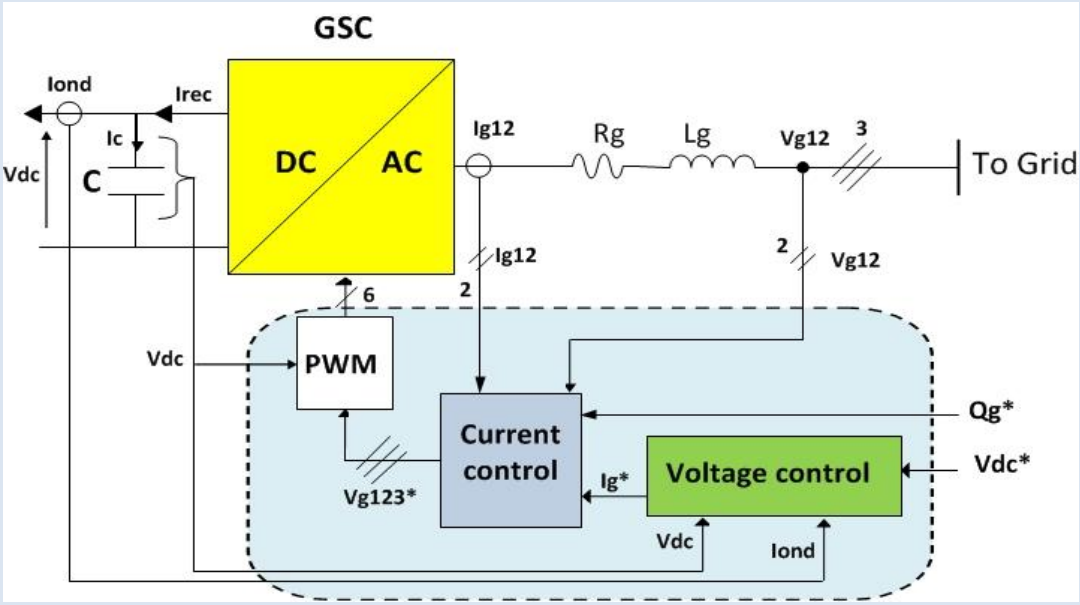

Fig 9 : Command approach of the Grid Side Converter (GSC)

As for the regulation of rotor currents, the model of the GSC converter is gain G equal to 1.

Block control loops of dq axes current scheme is described in Figure 10 . The regulators used are PI. In these block, diagrams control shows the compensation terms and dq axis decoupling and GSC models and link it to the network.

The reference dq-axis currents I_{gd}* and I_{gq}* are respectively provided in the block of the DC bus voltage control and reactive power control at the connection point of the GSC to the grid.

Active and reactive power exchanged with the electric network are given by the following relationships:

$$\begin{cases} P_g = V_{gd}.I_{gd} + V_{gq}.I_{gq} \\ Q_g = V_{gq}.I_{gd} - V_{gd}.I_{gq} \end{cases} \quad (25)$$

Neglecting the losses in the Rg resistance of RL filter and taking into account the orientation of the dq reference related to stator rotating field (V_{gd} = 0), the equations (25) becomes:

$$\begin{cases} P_g = V_{gq}.I_{gq} \\ Q_g = V_{gq}.I_{gd} \end{cases} \quad (26)$$

From these relations, it is possible to impose the active and reactive power reference, denoted by Pg* and Qg *, imposing reference currents I_{gd}* and I_{gq}*:

$$\begin{cases} I_{gq} *= \frac{P_g*}{V_{gq}} \\ I_{gd} *= \frac{Q_g*}{V_{gq}} \end{cases} \quad (27)$$

The direct current component is used to control the reactive power at the connection point of the GSC with the grid. The quadrature component is used to regulate the DC bus voltage. With this principle, a null reference of reactive power can be imposed (Q_g * = 0 VAr).

From equation (7), we can write the powers in the DC bus:

$$\begin{cases} P_{rec} = V_{dc}.I_{rec} \\ P_c = V_{dc}.I_c \\ P_{ond} = V_{dc}.I_{ond} \end{cases} \quad (28)$$

These powers are linked by the relation:

$$P_{rec} = P_c + P_{ond} \quad (29)$$

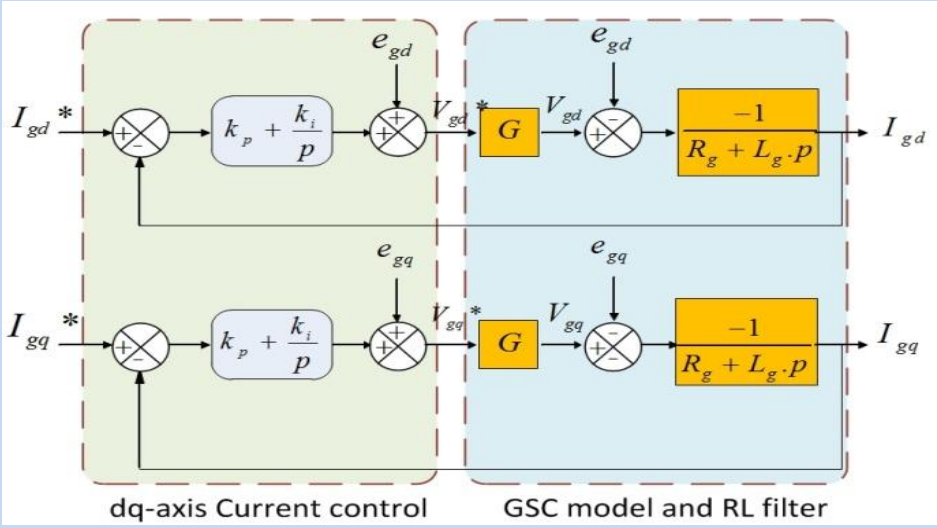

Fig 10 : dq-axis RL filter current control

If we neglect all Joule losses to the power exchanged between the rotor of the DFIG and the Grid (losses in the capacitor, the converter and the RL filter), we can write:

$$P_g = P_{rec} = P_c + P_{ond} \quad (30)$$

By adjusting the power Pg, it is possible to control the power Pc in the capacitor and thus regulate the DC bus voltage. To achieve this aim, the P_{ond} and Pc powers must be known to determine Pg *.

The reference power of the capacitor is connected to the current reference flowing in the capacitor:

$$P_c * = V_{dc}.I_c * \quad (31)$$

The regulation of the DC bus voltage is then effected by an external loop to maintain a constant voltage on the DC bus, with a PI corrector generating the reference current in the capacitor ic*.

Figure 11 shows the block diagram of the control of the DC bus voltage. We consider, (to simplify the control chain) the reference current I_{gq}* is always equal to the current I_{gq} because the response time of the inner loop is very small than that of the outer loop.

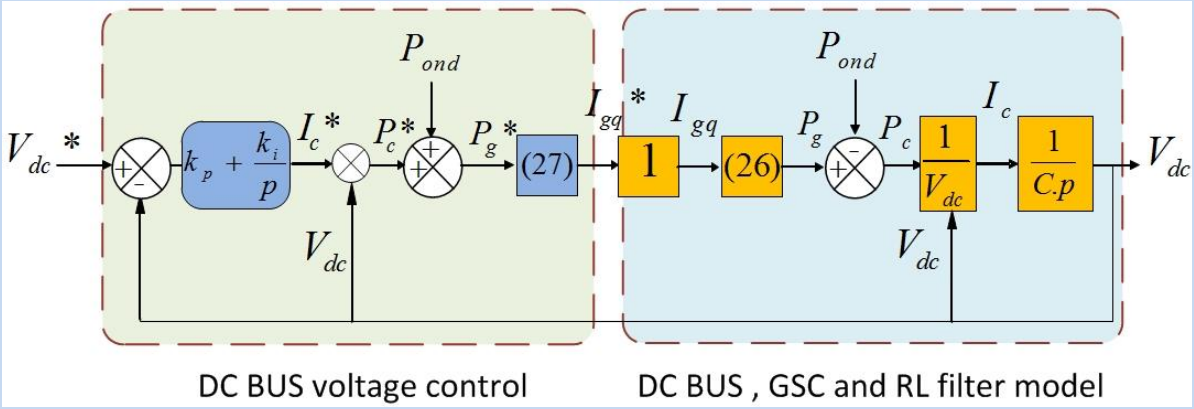

Fig 11 : DC BUS voltage control

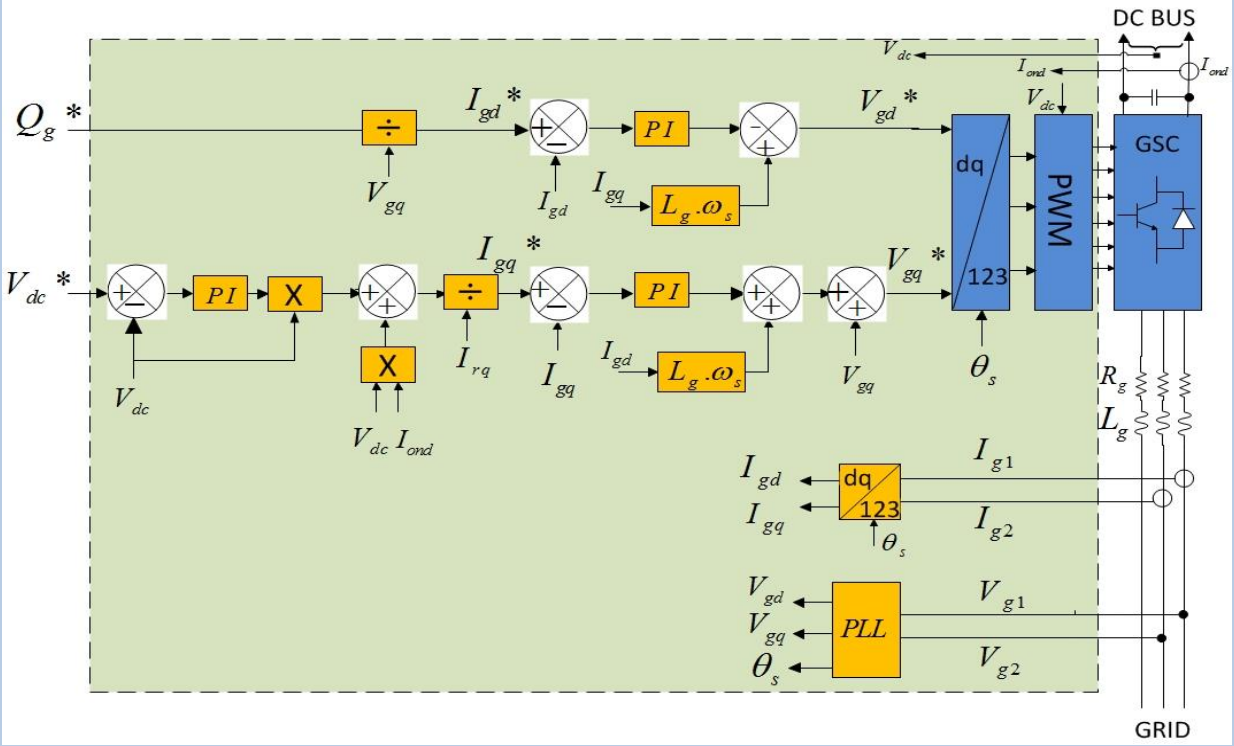

Fig 12 : Diagram block control of the Grid Side Converter

In Figure 11 P_{ond} corresponds to the rotor power: It is a considered as a regulation disturbance and will be compensated in the control chain.

Figure 12 shows the diagram block control of the GSC. This diagram includes the terms of decoupling and compensation in order to independently control the dq axes currents flowing in the RL filter and active and reactive power exchanged between the GSC and the electrical network.

IV. Simulation results

In this section, we present the choice of different parameters of the wind system based on DFIG and analyze the simulation results for the operating points characterized by a constant speed of the wind. We show that the various powers involved can be controlled independently.

Various electrical and mechanical parameters of the studied wind system are summarized in the following table:

The simulations were performed using Matlab/Simulink software. In order to validate the control approach discussed in this paper, we present an operating point when the wind speed is constant equal to 12m/s. For this simulation, we consider that the wind system is steady and produces maximum power as a function of wind speed.

System	Parameter
Turbine	Jt =1.4 10^6 kg.m^2, Vt_n =13m/s, R =40m
Multiplier	M = 100
DFIG	$U_s = U_r$ = 575V P_n = 3 Mw, f=50Hz, R_r =4mΩ, R_s=3mΩ, L_m= 12mH, L_s =120µH, L_r=50Mh, J_m=114kg.m^2 P =2
DC BUS	C=20mF, V_{dc}=1000V
RL Filter	R_g=0.1Ω, L_g= 0.6mH
GRID	U_g =575V, f=50Hz

The reference of the DC bus voltage denoted V_{dc}* is set at 1000V. The reference value of reactive power (Qg*) exchanged with the network through the converter GSC is set to (0VAr), which guarantees a power factor close to unity. The reactive power of stator Qs is regulated to reference value (Qs* = 0Var) in the control of RSC. The switching frequency of the power switches of the GSC and RSC is set to 10 kHz.

To validate our control approach, we applied a wind speed equal to 12 m/s on the blades of the wind, which corresponds to an operating speed of the DFIG in MPPT control about 1600 tr/min, as shown in Figure 13.a.

Figure 13.b shows the power extracted from the wind turbine which corresponds to a MPPT operation.

We also observe in Figure 13.c that the DC bus voltage is well regulated to 1000 V.

Figure 13.d shows the active and reactive power in the stator of the DFIG. We note that the active power extracted from the wind turbine is injected into the network and the reactive power is controlled to zero. Fig 13.e illustrate a zoom of the reactive stator power.

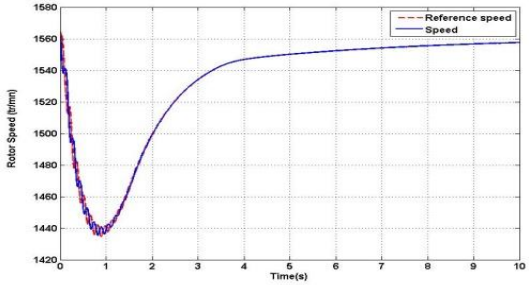

(a) Operating speed of the DFIG

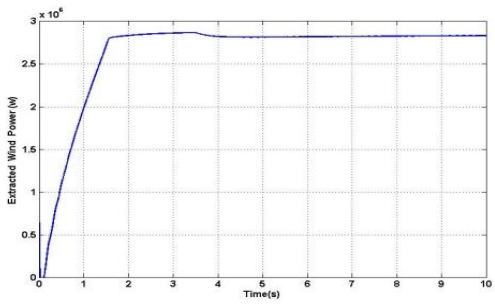

(b) Extracted power of the wind turbine

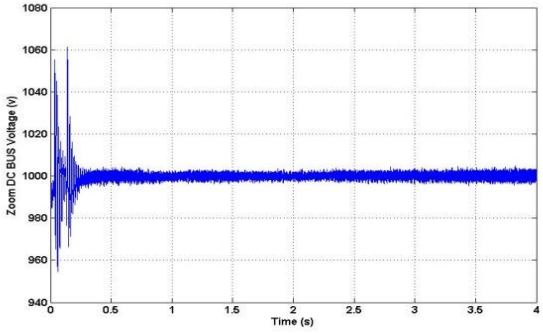

(c) DC bus Voltage

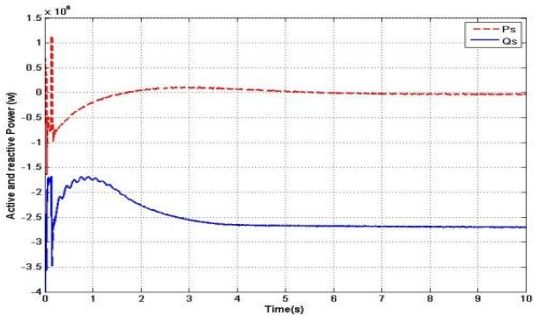

(d) Active and reactive power in the stator of the DFIG (Ps and Qs)

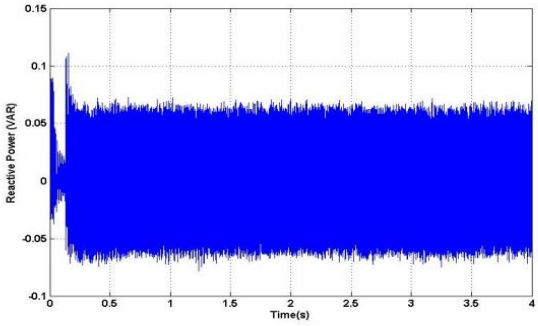

(e) Zoom of the reactive power Qs

Fig 13 : simulations results

V. Conclusion

This paper has addressed the modeling and control of a wind system with constant speed of the wind based on a DFIG. At first, we explained why this wind system is the most used now including the economy realized through the design of static converters implemented.

Then we are interested in modeling of various components of wind system. In fact, the aerodynamic and mechanical models of the turbine have been developed. Then, in order to establish different controllers of two

converters, we have developed models of DFIG and Liaison of the GSC to the network via the RL filter.

In the rest of this paper, we considered that the wind was in its optimum range of operation and it worked steady regardless of the wind speed applied to the blades. We have focused our study on the control in this area of operation allowing the wind to extract the maximum power available. We used an indirect method of MPPT control without adjustment of the rotational speed. The various controls of GSC and RSC were detailed to provide independent control of active and reactive power while ensuring optimal operation of the turbine.

To validate the modeling and control of the global wind system, we have performed a simulation for an operating point at constant wind speed. The results showed that the active and reactive power of the wind system based on the DFIG could be controlled independently while ensuring optimal active power supplied to the grid.

Bibliographies :

[1] Vijay Chand Ganti, Bhim Singh, Shiv Kumar Aggarwal, and Tara Chandra Kandpal, DFIG-Based Wind Power Conversion With Grid Power Leveling for Reduced Gusts, IEEE TRANSACTIONS ON SUSTAINABLE ENERGY, VOL. 3, NO. 1, JANUARY 2012

[2] BY S . Muller, M. Deicke, Rikw. De Doncker, doubly fed induction generator systems, IEEE Industry Applications Magazine May | June 2002

[3] J. B. Ekanayake, L. Holdsworth, X. G. Wu, and N. Jenkins, "Dynamic modeling of doubly fed induction generator wind turbines," IEEE Trans. Power Syst., vol. 18, no. 2, pp. 803–809, May 2003.

[4] Jun Yao, Hui Li, Yong Liao, and Zhe Chen, An Improved Control Strategy of Limiting the DC-Link Voltage Fluctuation for a Doubly Fed Induction Wind Generator, IEEE TRANSACTIONS ON POWER ELECTRONICS, VOL. 23, NO. 3, MAY 2008

[5] Yufei Tang, Ping Ju, HaiboHe, Chuan Qin, and Feng Wu, Optimized Control of DFIG-Based Wind Generation Using Sensitivity Analysis and Particle Swarm Optimization, IEEE TRANSACTIONS ON SMART GRID, VOL. 4, NO. 1, MARCH 2013

[6] Mohamed Benbouzid, Brice Beltran, Yassine Amirat, Gang Yao, Jingang Han and Hervé Mangel, High-Order Sliding Mode Control for DFIG-Based Wind Turbine Fault Ride-Through, IEEE IECON 2013, Vienne, Austria 2013

[7] Yateendra Mishra, S. Mishra, Fangxing Li, Zhao Yang Dong, and Ramesh C. Bansal, Small-Signal Stability Analysis of a DFIG-Based Wind Power System Under Different Modes of Operation, IEEE TRANSACTIONS ON ENERGY CONVERSION, VOL. 24, NO. 4, DECEMBER 2009

[8] M. Itsaso Martinez, Ana Susperregui, Gerardo Tapia Haritza Camblong, Sliding-Mode Control for a DFIG-based Wind Turbine under Unbalanced Voltage, 18th IFAC World Congress Milano (Italy) August 28 - September 2, 2011

[9] A. Petersson, L. Harnefors, and T. Thiringer, "Evaluation of current control methods for wind turbines using doubly-fed induction machines," IEEE Trans. Power Electron., vol. 20, no. 1, pp. 227–235, Jan. 2005.